

1 **The impact of the afternoon planetary boundary-layer height on the**
2 **diurnal cycle of CO and CO₂ mixing ratios at a low-altitude**
3 **mountaintop**

4
5 **Temple R. Lee, Stephan F. J. De Wekker, and Sandip Pal**

6
7
8 Received: 22 January 2018 / Accepted: xx xx xx
9

10 **Abstract:** Mountaintop trace-gas mixing ratios are oftentimes assumed to represent free-
11 atmospheric values, but are affected by valley planetary boundary-layer (PBL) air at certain
12 times. We hypothesize that the afternoon valley-PBL height relative to the ridgetop is important
13 in the diurnal cycle of mountaintop trace-gas mixing ratios. To investigate this, we use, 1) four-
14 years (1 January 2009 – 31 December 2012) of CO and CO₂ mixing-ratio measurements and
15 supporting meteorological observations from Pinnacles (38.61 °N, 78.35 °W, 1017 m a.s.l.),
16 which is a monitoring site in the Appalachian Mountains, 2) regional O₃ mixing-ratio
17 measurements, and 3) PBL heights determined from a nearby sounding station. Results reveal
18 that the amplitudes of the diurnal cycles of CO and CO₂ mixing ratios vary as a function of the
19 daytime maximum valley-PBL height relative to the ridgetop. The mean diurnal cycle for the
20 subset of days when the afternoon valley-PBL height is at least 400 m below the ridgetop shows

Temple R. Lee*; Stephan F. J. De Wekker; Sandip Pal, Department of Environmental Sciences,
University of Virginia, 291 McCormick Road, Charlottesville, VA 22904
e-mail: temple.lee@noaa.gov

*Now at NOAA ARL Atmospheric Turbulence and Diffusion Division and [Cooperative Institute for Mesoscale Meteorological Studies](#), 456 S. Illinois Avenue, Oak Ridge, TN 37830

21 a daytime CO mixing-ratio increase, implying the transport of PBL air from the valley to the
22 mountaintop. During the daytime, on days when the PBL heights exceed the mountaintop, PBL
23 dilution and entrainment cause CO mixing ratios to decrease. This decrease in CO mixing ratio,
24 especially on days when PBL heights are at least 400 m above the ridgetop, suggests that
25 measurements from these days can be used as with afternoon measurements from flat terrain in
26 applications requiring regionally-representative measurements.

27

28 **Keywords:** Carbon dioxide; Carbon monoxide; Mountaintop monitoring; Planetary boundary-
29 layer height

30

31 **1 Introduction**

32 Mixing processes within the planetary boundary layer (PBL) affect the exchange of heat,
33 moisture, momentum, trace gases, and aerosols between the Earth's surface and adjacent free
34 atmosphere (e.g. Stull 1988). The PBL height represents the height to which these turbulent
35 mixing processes occur. Over flat terrain and assuming a higher trace-gas mixing ratios in the
36 PBL than in the overlying free atmosphere, growth of the daytime PBL causes free atmospheric
37 air to be entrained into the PBL, causing mixing ratios of passive trace gases to decrease (e.g.
38 Pochanart et al. 2003, Elankaty et al. 2007, Popa et al. 2010, Pal 2014, Pal et al. 2015, Berhanu et
39 al. 2016, Chandra et al. 2016, Sreenivas et al. 2016). For this reason, the PBL height is an
40 essential parameter describing the vertical mixing of trace gases and pollutants in air quality
41 dispersion studies (e.g. Dabberdt et al. 2004, Koffi et al. 2016).

42 Over mountaintops, the relationship between PBL height and the diurnal cycle of aerosols
43 and trace gases is more complex because of local and mesoscale transport processes occurring in
44 these areas (e.g. Rotach and Zardi, 2007, van der Molen and Dolman, 2007, De Wekker et al.

45 2009, Steyn et al. 2013, Pal et al. 2014, 2016). Thus, the diurnal cycle of trace-gas species,
46 assuming that there are no local sources or sinks affecting the trace-gas mixing ratio, is governed
47 by the trace-gas mixing ratio over the surrounding lower terrain via vertical and horizontal
48 mixing. Consequently, the diurnal trace-gas cycle over mountaintops is much different than over
49 flat terrain. In situations when the valley-PBL top remains below the mountaintop, there is
50 oftentimes no clear diurnal trace-gas cycle. In these situations, mountaintop trace-gas mixing
51 ratios are often assumed to be representative of free-atmospheric mixing ratios, as has been
52 shown in trace gas and aerosol observations from tall mountaintops (e.g. Baltensperger et al.
53 1997, Lugauer et al. 1998).

54 In other situations, PBL air in adjacent valleys has a significant impact on the mountaintop
55 trace-gas cycle. During the daytime, polluted PBL air from within the valley is transported to the
56 mountaintop via growth of the valley PBL and thermally-driven upslope flows. Previous studies
57 have found that these processes influence the diurnal cycle of carbon dioxide (CO₂) mixing-
58 ratios observed at nearby mountaintops (e.g. Keeling et al. 1976, Thoning et al. 1989, De
59 Wekker et al. 2009) and affect the presence of the daytime minimum CO₂ mixing-ratio (e.g. De
60 Wekker et al. 2009; Pal et al., 2017). Other trace gas and aerosol species exhibit an increase in
61 mixing-ratio at mountaintop sites due to the arrival of valley-PBL air at the mountaintop via
62 growth of the valley PBL and thermally-driven upslope flows. The observed increase has been
63 reported for many trace-gas species, including carbon monoxide (CO) (e.g. Weiss-Penzias et al.
64 1996, Forrer et al. 2000, Lin et al. 2011, MacDonald et al. 2011), ozone (O₃) (e.g. Sullivan et al.
65 2016), methane (e.g. Necki et al. 2003; Bamberger et al. 2017), gaseous mercury (e.g. Obrist et
66 al. 2008), as well as aerosols (e.g. Baltensperger et al. 1997, Bukowiecki et al 2016). The
67 [amplitude](#) and timing of this increase vary seasonally. The increase is typically largest during the

68 summer when the valley PBL is deep and exceeds the mountaintop height, but may be non-
69 existent during the winter when the valley PBL is very shallow and remains below the
70 mountaintop. In the latter scenario, the mountaintop remains in the free atmosphere throughout
71 the day (e.g. Baltensperger et al. 1997, Lugauer et al. 1998, Henne et al. 2008a, Henne et al.
72 2008b). Oftentimes, there is a corresponding night-time decrease in CO mixing ratio (e.g. Gao et
73 al. 2005, Balzani Lööv et al. 2008, Henne et al. 2008b) and aerosols (e.g. Baltensperger et al.
74 1997, Bukowiecki et al 2016) because sinking motions transport free-atmospheric air to the
75 mountaintop (e.g. Schmidt et al. 1996).

76 Identifying representative measurements is important for a number of applications including,
77 e.g. atmospheric chemistry studies (e.g. Novelli et al. 1998), air quality studies (e.g. Dabbert et
78 al. 2004), and carbon cycle studies (e.g. Andrews et al. 2014). One of the simplest filtering
79 approaches is to remove measurements made during the daytime and only assimilate night-time
80 measurements from mountaintops (e.g. those made between 0000 and 0400 local standard time
81 [LST]) into these applications (e.g. Peters et al. 2010). The major assumption of this approach is
82 that night-time measurements made at mountaintops are representative of the free atmosphere
83 (e.g. Schmidt et al., 1996). In addition to filtering trace-gas measurements by time of day,
84 statistical filtering techniques, e.g. removing outliers, using low-pass filters (e.g. Thoning et al.
85 1989), filtering measurements made when there are strong local vertical trace-gas gradients and
86 excessive hourly variances present in the measurements (e.g. Brooks et al. 2012), have been
87 developed to identify regionally-representative trace-gas measurements. Meteorological analyses
88 have also been used to identify measurements affected by local sources, including performing
89 trajectory analyses to identify source regions of elevated trace-gas mixing ratios (e.g. Forrer et al.
90 2000, Zellwegger et al. 2003), and distinguishing between upslope and downslope flows using in

91 situ meteorological measurements (e.g. Henne et al. 2008a). However, to the best of our
92 knowledge, no study has used knowledge of daytime PBL heights to identify regionally-
93 representative trace-gas measurements from mountaintops.

94 Following the aforementioned studies, one may hypothesize that the diurnal trace-gas cycle
95 at mountaintops depends on the maximum daytime PBL height in the adjacent low-lying terrain
96 relative to the ridgetop height. This dependency can then be used in helping identify regionally-
97 representative mountaintop trace-gas measurements. Recent studies have begun to address this
98 hypothesis using mountaintop CO mixing ratio and accompanying in situ meteorological
99 measurements. Lee et al. (2015) found that, for a mountaintop site in north-western Virginia,
100 USA, referred to as the Pinnacles site, CO mixing ratios decreased during the daytime on clear
101 fair weather days. Pollutants contained within the valley PBL arrived at the mountaintop in these
102 cases, but PBL mixing and dilution effects produced a decrease in mountaintop CO mixing
103 ratios.

104 In the present study, we follow up on these analyses by investigating how these mountaintop
105 trace gas changes depend on the daytime maximum PBL height relative to the ridgetop height.
106 We address this question for both CO and CO₂ mixing ratios and use four years of measurements
107 accompanied by collocated meteorological measurements from the Pinnacles site and also
108 meteorological measurements from surrounding locations. These measurements allow for a
109 process-based study, rather than a climatological overview of the trace-gas measurements at the
110 Pinnacles site that previous studies have provided (i.e. Lee et al. 2015). The Pinnacles site is an
111 ideal location to investigate the influence of the PBL height relative to the ridgetop on the
112 observed trace-gas cycle because the PBL height can either be well below or well above the
113 ridgetop (e.g. Lee and De Wekker 2016). Furthermore, the CO₂ mixing-ratio measurements from

114 the Pinnacles site are currently used to estimate regional- to continental-scale carbon fluxes in
115 CarbonTracker, an inverse carbon transport model that assimilates observations from regionally-
116 representative trace-gas monitoring sites located in flat terrain (e.g. Peters et al. 2007) and at
117 mountaintops (e.g. Lin et al. 2017). Careful selection of trace-gas measurements and their degree
118 of representativeness from sites such as Pinnacles is necessary to improve the surface fluxes
119 calculated by these models.

120

121 **2 Site Description and Datasets**

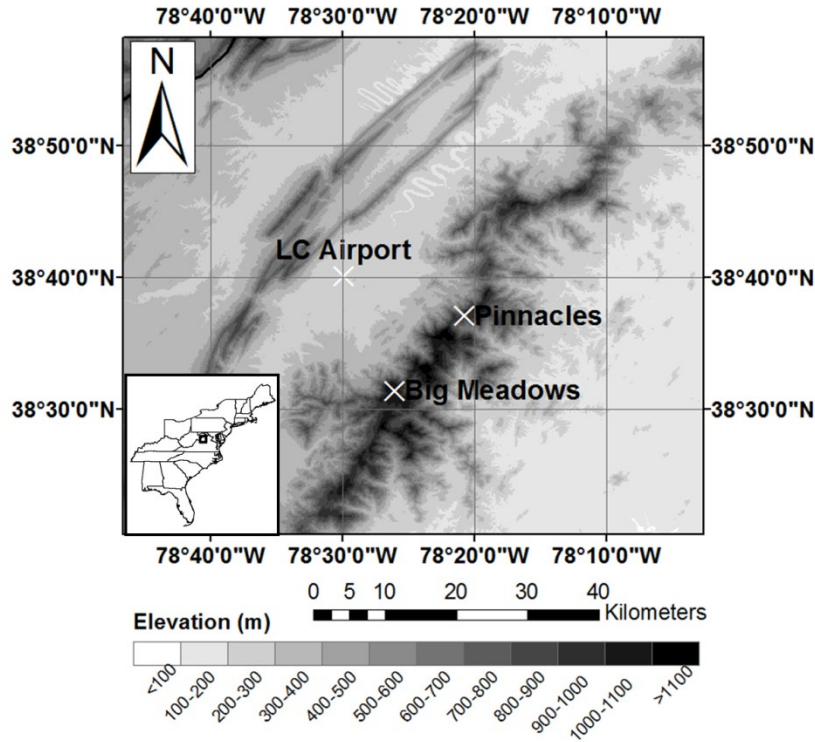
122 2.1 Site Description

123 The Pinnacles site (38.61 °N, 78.35 °W, 1017 m above sea level (a.s.l.)) is a mountaintop site
124 with a 17-m tower from which meteorological and trace-gas measurements have been made
125 since 2008. The site is located in the Virginia Blue Ridge Mountains, which are along the eastern
126 flank of the Appalachians in the eastern USA. The mountain ridge on which the Pinnacles site is
127 located ranges in height from 1000 to 1200 m a.s.l. and is about 800 m above the surrounding
128 valley and plain. The Page Valley, part of the larger Shenandoah Valley, is located west of the
129 Pinnacles site; the Virginia Piedmont is located east of the Pinnacles site. The area immediately
130 surrounding the Pinnacles site is a mixed deciduous forest with a mean canopy height of about
131 14 m, while the adjacent lowlands are comprised of mixed deciduous forests and cropland.
132 Further details about the site and surrounding region are found in, e.g. Lee et al. (2012) and Lee
133 et al. (2014).

134

135 2.2 CO Mixing-Ratio Measurements

136 CO and CO₂ mixing-ratio measurements at the Pinnacles site began in late August 2008 at 5, 10,
137 and 17 m a.g.l. (above ground level) through a collaboration with the NOAA Earth System
138 Research Laboratory. The measurement system and in situ calibrations have already been
139 described by Lee et al. (2015), and a detailed description of the measurement uncertainties is
140 discussed in Andrews et al. (2014). In the present study, we used 30-min means of the CO and
141 CO₂ mixing-ratio data collected 17 m a.g.l. during the site's first four full years of operation, i.e.
142 1 January 2009 through 31 December 2012. Much of our focus is on CO mixing ratio rather than
143 CO₂ mixing ratio because, during the growing season, CO₂ mixing ratio is affected both by PBL-
144 dilution and entrainment as well as photosynthetic uptake occurring on site and along upwind
145 forested mountain slopes (e.g. Sun et al. 2007), which complicate the interpretation of the diurnal
146 cycle. Because CO mixing ratio is unaffected by local uptake, it is a more suitable candidate than
147 CO₂ mixing ratio for investigating PBL mixing and transport processes over mountainous terrain.
148



149

150 **Fig 1** Topographic map indicating the location of the Pinnacles site relative to the Big Meadows site and the Luray
 151 Caverns (LC) airport (white X's). Shading shows elevation a.s.l. The inset map at the bottom left indicates the study
 152 location, denoted by a black box, in the eastern USA.

153

154 2.3 Supplemental Measurements

155 To help interpret the diurnal CO and CO₂ mixing-ratio cycle, we used supplemental
 156 meteorological and trace-gas measurements. Meteorological measurements at the Pinnacles site
 157 began in July 2008 and include temperature, humidity, wind speed and direction, rainfall,
 158 pressure, incoming and outgoing shortwave and longwave radiative fluxes, and fluxes of sensible
 159 heat, latent heat, and CO₂ mixing ratio. In addition to measurements from the Pinnacles site, we
 160 used meteorological and trace-gas measurements from nearby monitoring sites. Mountaintop O₃
 161 mixing-ratio measurements were obtained from the Big Meadows site (38.52 °N, 78.44 °W,
 162 1079 m a.s.l.), located on the same ridgeline 14 km south of the Pinnacles site, and from the Page

163 Valley (Fig. 1) at the Luray Caverns airport (38.66 °N, 78.50 °W, 275 m a.s.l.), located 13 km
164 west of the Pinnacles site. At both the Big Meadows site and the Luray Caverns airport, O₃
165 mixing ratios were measured 10 m a.g.l. using a Thermo Environmental Instruments Model 49i
166 UV photometric O₃ analyzer that has a 1-ppb precision, a 20-s response time, and span drift of
167 <1%. The data record at the Big Meadows site for the period of interest was mostly complete,
168 although there existed a data gap between late February and April 2010. At the Luray Caverns
169 airport, hourly O₃ mixing ratios were sampled from 1 April through 31 October annually.

170

171 **3 Methods**

172 3.1 Determining PBL Heights near the Mountaintop

173 Reliable PBL height estimates over the Page Valley, which is most often upwind of the Pinnacles
174 site based on previous studies of the site's climatology (e.g. Lee 2015; Lee et al. 2015), are
175 required to investigate the role of the valley PBL on the trace-gas cycle at the Pinnacles site. In
176 the Page Valley, there exists no PBL height observations for the entire period of interest. One
177 approach is to assume that PBL heights obtained from a nearby sounding station, where twice-
178 daily rawinsonde observations are made, are representative of the region (e.g. Hondula et al.
179 2013). However, the spatial variability in PBL heights needs to be carefully assessed when using
180 this approach. Lee and De Wekker (2016) found that mean afternoon PBL heights over the Page
181 Valley are 200-400 m larger than the PBL heights estimated using observations from the nearest
182 sounding station, located at Dulles airport (38.98 °N, 77.49 °W, 87 m a.s.l.) 90 km north-east of
183 the Page Valley. Greater PBL heights over the Page Valley than near Dulles airport arise due to
184 higher terrain and drier conditions in the Page Valley. Accounting for these PBL height
185 differences is necessary to obtain the most reliable PBL height estimates for the Page Valley.
186 Thus, to estimate PBL heights over the Page Valley, we used 0000 UTC (UTC = LST + 5)

187 Dulles airport rawinsonde observations and followed the approach developed by Lee and De
188 Wekker (2016) to remove the early-evening near-surface stable layer oftentimes present in the
189 sounding. We then calculated the bulk Richardson (R_b) number and determined the afternoon
190 PBL height at Dulles airport as the first height where R_b exceeded a critical threshold, R_c , which
191 we set to 0.25 (Vogelezang and Holtslag, 1996). The approach has been found to yield PBL
192 heights that agree well with afternoon PBL heights obtained from reanalysis products and
193 aircraft observations (i.e. Lee and De Wekker 2016) and has recently been used to develop a
194 climatology of afternoon PBL heights over the contiguous USA (Lee and Pal 2017).

195 To determine PBL heights over the Page Valley site from the afternoon Dulles Airport PBL
196 height, following Lee and De Wekker (2016), we computed the difference in the daily 2100 UTC
197 PBL height between the grid box in the North American Regional Reanalysis (Mesinger et al.
198 2006) containing the Page Valley and the grid box containing Dulles Airport for the period 2009-
199 2012. Based on the analyses presented in Lee and De Wekker (2016), we determined a seasonal
200 correction factor that represents the mean difference in PBL height as a function of season (Table
201 1) and applied this correction to the afternoon PBL heights estimated from the 0000 UTC
202 rawinsonde at Dulles Airport.

203

204 3.2 Interpreting Mountaintop Trace-gas Measurements

205 To help interpret the mountaintop trace-gas diurnal cycles, we subtracted the daily mean from
206 each day before averaging the values together to generate composites. Removing the daily means
207 allows for a better investigation of the dominant physical processes affecting the daily trace-gas
208 cycle on diurnal time scales and removes the major influence of processes affecting trace-gas
209 mixing ratios at longer time scales. For CO_2 mixing ratio, these processes include the seasonal

210 cycle in vegetative photosynthetic uptake and respiration (e.g. Lee et al. 2012), whereas the
211 seasonality of hydroxyl radicals and anthropogenic emissions affects the seasonal cycle in CO
212 mixing ratio (e.g. Thompson et al. 1992; Novelli et al. 1998).

213 Once we removed the daily means and calculated the standard errors (*SE*), we investigated
214 the role of the PBL height on the diurnal CO₂ and CO mixing ratio cycle for all days, regardless
215 of the presence or absence of a wind-direction shift. Distinguishing between days with wind-
216 direction shifts and days without wind-direction shifts is important because of the role that wind-
217 direction shifts have on the observed trace-gas cycle at the site (Lee et al. 2015). The wind
218 climatology from the site shows a backing from the north-west in the early morning to the south-
219 west during the daytime. This wind-direction shift occurs on a regional scale and is not a result
220 of local, thermally-driven flows. The wind-direction shift has been found to correlate with trace-
221 gas cycle (in particular an increase in CO mixing ratio which makes it difficult to isolate the role
222 of PBL height on the diurnal CO and CO₂ mixing ratio cycle. Thus, following Lee et al. (2015),
223 we also identified days without a wind-direction shift and that also had clear skies, using a
224 clearness index (e.g. Whiteman et al. 1999), and compared these days to the set of days that
225 included cloudy days and days with wind-direction shifts.

226 Because the uncertainties in monthly PBL height estimates in this region can be as large as
227 400 m (Lee and De Wekker 2016), we classified days with PBL heights below the ridgetop when
228 the PBL height was at least 400 m below the maximum height of the mountain ridge (1200 m),
229 and we classified days with PBL heights above the ridgetop when the PBL height was at least
230 400 m above the ridgetop height. Thus, days with PBL heights <800 m a.s.l. and >1600 m a.s.l.
231 were classified as below the ridgetop and above the ridgetop, respectively. Altering these

232 threshold values by ± 200 m did not significantly affect the mean diurnal CO or CO₂ mixing-ratio
233 cycles on these subsets of days.

234 To understand the role of valley-PBL air on the diurnal CO and CO₂ mixing-ratio cycles, we
235 used mountaintop measurements of specific humidity (q) and mountaintop and valley
236 measurements of O₃ mixing ratio. We used O₃ mixing ratio and specific humidity measurements
237 since they can be used as tracers of PBL air (e.g. Weiss-Penzais et al. 2006) and because CO and
238 CO₂ mixing-ratio measurements were unavailable from the valley. We computed differences in
239 O₃ mixing ratio between the mountaintop and valley to discern valley-PBL influences on the
240 mountaintop measurements. Large O₃ mixing-ratio differences (e.g. >20 ppb) imply less
241 influence of valley-PBL air on the mountaintop measurements; small O₃ mixing-ratio differences
242 (e.g. \approx zero) suggest that valley-PBL air reaches the mountaintop and affects the mountaintop
243 trace-gas measurements.

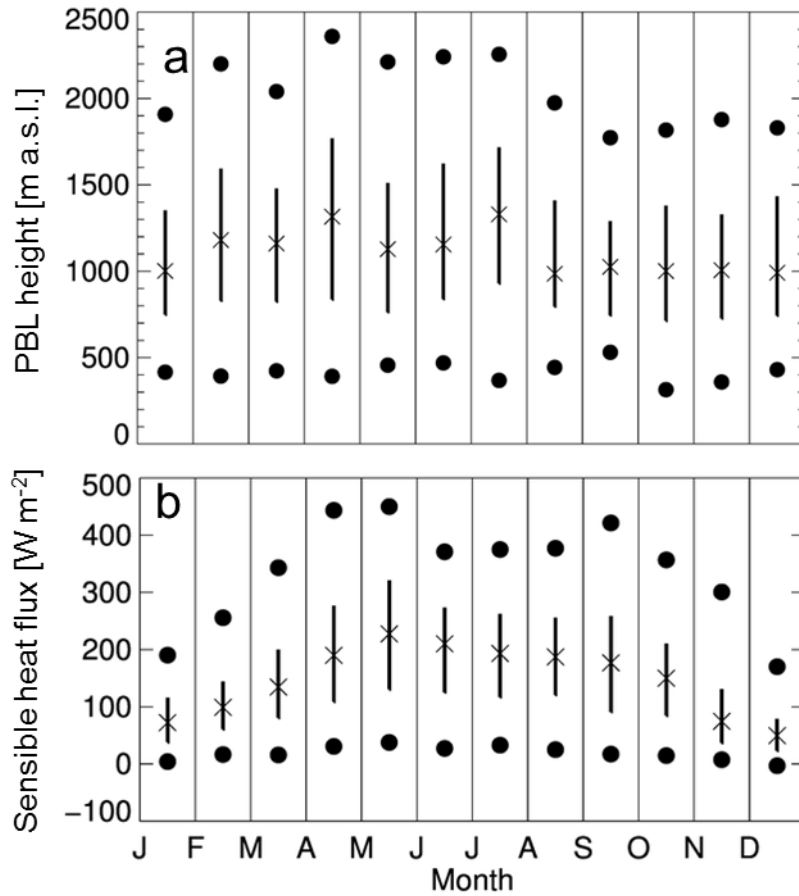
244

245 **4 Results**

246 4.1 Seasonal PBL Height Cycle

247 During the four-year period of interest, PBL heights in the 0000 UTC Dulles airport sounding
248 range from <500 m a.s.l. to >2500 m a.s.l. (Fig. 2a). PBL heights range from 500 to 2000 m a.s.l.
249 in the winter, with mean values around 1000 m a.s.l. PBL heights are largest in the spring and
250 summer, when maximum values are around 2300 m a.s.l. The seasonal cycle in PBL heights
251 closely follows the seasonal cycle of sensible heat flux and has been investigated in previous
252 work (Lee and De Wekker, 2016). Afternoon (1200-1600 LST) sensible heat flux computed at
253 the Pinnacles site is typically 50 W m^{-2} in the winter when PBL heights are smallest, but is
254 largest in the late spring and early summer when mean afternoon sensible heat flux is typically
255 around 200 W m^{-2} (Fig. 2b). In the discussion that follows, we consider situations in which the

256 PBL heights are well below or well above the ridge height, i.e. <800 m a.s.l. and >1600 m a.s.l.,
 257 respectively. Over the total 4-year period, these situations occurred 24% and 32% of the time,
 258 respectively, for all days (i.e. regardless of if the day was cloudy or if there was a wind-direction
 259 shift present).



260
 261 **Fig 2** PBL height percentiles, computed over the period 1 January 2009 – 31 December 2012, as a function of time
 262 of year after removing the near-surface stable layer from the 0000 UTC Dulles airport sounding following Lee and
 263 De Wekker (2016) (a). Panel (b) shows afternoon (1200-1600 LST) the sensible heat flux from the Pinnacles site.
 264 X's indicate medians; black bars extend out to the 25th and 75th percentiles. Dots indicate 5th and 95th percentiles.
 265 The sensible heat flux is the mean over eight 30-min averages between 1200 and 1600 LST, whereby the first
 266 average is from 1200-1230 LST and the final 30-min average is from 1530-1600 LST.

267 4.2 Overview of CO and CO₂ Mixing-Ratio Measurements

268 The mean seasonal and diurnal cycles of CO mixing ratio at the Pinnacles site have been
269 described in previous work (Lee et al. 2015), and characteristics of the mean seasonal and
270 diurnal CO₂ mixing-ratio cycle have been described by Lee et al. (2012) and Lee (2015). Briefly,
271 CO mixing ratios are typically highest in March and lowest in October (not shown) which is
272 consistent with findings from other mid-latitude continental monitoring sites (e.g. Popa et al.
273 2010, Cristofanelli et al. 2013). The mean diurnal CO mixing-ratio cycle at the Pinnacles site is
274 characterized by a daytime CO mixing-ratio increase, which is a common feature of other
275 mountaintop monitoring sites at which valley-PBL air affects mountaintop trace-gas mixing-
276 ratios (e.g. Atlas and Ridley, 1996, MacDonald et al. 2011). The CO mixing-ratio increase
277 occurs in all seasons and has the smallest amplitude in the summer (4.0 ppb) and largest
278 amplitude in the winter (7.1 ppb) (Lee et al. 2015), which is inconsistent with the diurnal CO
279 mixing-ratio cycle at mountaintops taller than Pinnacles (e.g. Forrer et al. 2000, Henne et al.
280 2008b, Ou-Yang et al. 2014). At mountaintops taller than Pinnacles, deeper PBL heights during
281 the summer than during the winter allow for valley-PBL air to be transported to the mountaintop,
282 causing the largest CO mixing-ratio increases during the summer. Additionally, previous work at
283 the Pinnacles site has found large day-to-day CO mixing-ratio variability which arises due to
284 synoptic scale transport (Lee et al. 2012) and mesoscale circulations (Lee et al. 2015).

285 In contrast to CO mixing ratio, previous studies on CO₂ mixing ratio at the Pinnacles site
286 have shown that seasonal changes are strongly correlated with seasonal changes in uptake and
287 respiration (Lee et al. 2012). Consistent with other continental locations (e.g. Greco and
288 Baldocchi 1996; Schmidt et al. 2014; Berhanu et al. 2016; Chandra et al. 2016; Sreenivas et al.
289 2016), mean CO₂ mixing ratios are typically highest in winter and lowest in the summer. On

290 diurnal time scales, there is a daytime decrease caused by local to regional photosynthetic uptake
291 occurring during the growing season. There is also large day-to-day variability in CO₂ mixing
292 ratios due to mesoscale to synoptic scale transport processes that result in hourly CO₂ mixing-
293 ratio changes sometimes exceeding 20 ppm (Lee et al. 2012) which is in agreement with findings
294 reported at other forested mountaintop monitoring sites (e.g. Pillai et al. 2011; Brooks et al.
295 2012).

296

297 4.3 Effect of PBL Height on the Diurnal CO and CO₂ Mixing-Ratio Cycle

298 4.3.1 CO Mixing-Ratio Diurnal Cycle

299 We found significant differences in the mean diurnal CO mixing-ratio cycle that depend on, 1)
300 whether the PBL is below the ridgetop or the PBL is above the ridgetop, and 2) whether or not
301 the day is a fair weather day with constant wind directions (Fig. 3). The same diurnal trends are
302 found when computing the medians; in the present paper, we discuss the diurnal trends in the
303 means for consistency with previous work at the site (e.g. Lee et al. 2012, Lee et al. 2015). When
304 all days are considered (i.e. independent of the presence of fair weather conditions or presence of
305 a wind-direction shift at the site), there is a daytime increase in the mean diurnal CO mixing-
306 ratio cycle on days when the PBL height is below 800 m a.s.l. On these days, CO mixing ratios
307 increase from a minimum around 0700 LST to a maximum at 1900 LST (Fig. 3a). In contrast,
308 daytime CO mixing ratios show a small decrease when the PBL height is above 1600 m a.s.l.,
309 but both cases show nearly constant CO mixing ratios after 1900 LST that suggest that the
310 mountaintop is sampling air from the residual layer or the free atmosphere.

311 Notable differences are present when we selected fair weather days with constant wind
312 directions (Fig. 3b), i.e. days on which we expect there to be the largest sensitivity in trace-gas
313 variability to differences in PBL height. Whereas the [amplitude](#) of the CO mixing-ratio increase

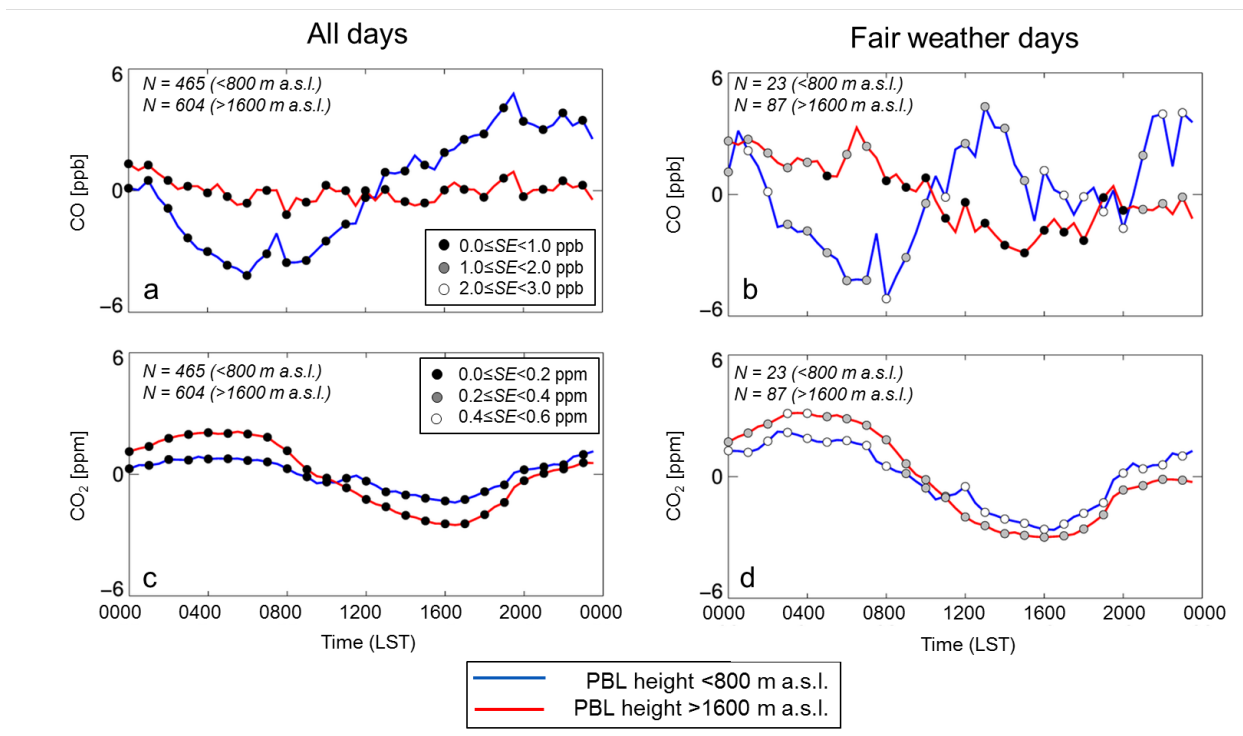
314 on days when the PBL height is below the ridgetop is comparable between all days and fair
315 weather days with constant wind directions (9.5 ppb vs 9.0 ppb), CO mixing ratios on fair
316 weather days with PBL heights below the ridgetop height decrease following a 1300 LST
317 maximum. Additionally, on days with PBL heights above the ridgetop height, the mean decrease
318 (6.2 ppb) is larger on fair weather days with constant wind directions (c.f. Fig. 3b) than the mean
319 decrease for all days (c.f. Fig. 3a). On these days with a large afternoon decrease in CO mixing
320 ratios, PBL dilution and entrainment cleaner free atmospheric air is likely to be the dominant
321 driver of the diurnal CO mixing-ratio cycle, as shown in recent case studies from the site (Pal et
322 al. 2017). Also, we note that the diurnal changes on these sets of days, including the short-lived
323 peak around 1300 LST on days with a shallow PBL, are much larger than the standard errors.

324

325 4.3.2 CO₂ Mixing-Ratio Diurnal Cycle

326 In the case of CO₂ mixing ratios, there is a decrease during the daytime both on days when the
327 PBL height is below the ridgetop and on days when the PBL height is above the ridgetop,
328 regardless of whether or not fair weather days are considered (Fig. 3c; Fig. 3d). Maximum CO₂
329 mixing ratios are observed between 0200 LST and 0600 LST, whereas the minimum in CO₂
330 mixing ratios occurs around 1600 LST. When the PBL is below the ridgetop, the amplitude of
331 the diurnal CO₂ mixing-ratio cycle is 2.5 ppm when all those days are considered, but is 4.8 ppm
332 on fair weather days with constant wind directions. Uncertainties are small on both subsets of
333 days compared with the amplitude of the changes in the mean cycles; standard errors are <0.6
334 ppm for both subsets of days. In addition, both subsets of days with PBL heights below the
335 ridgetop have a short-lived CO₂ mixing-ratio increase around noon. However, there is no such
336 increase when the PBL exceeds the ridgetop. When all days with PBL heights exceeding the

337 ridgetop are considered, the **amplitude** of the mean diurnal cycle is 4.6 ppm, but is 6.1 ppm on
 338 fair weather days with constant wind directions. We attribute the larger **amplitude** of the mean
 339 diurnal CO₂ mixing-ratio cycle on fair weather days to a combination of mixing within the
 340 daytime PBL and also to greater uptake occurring both at the site and along upwind forested
 341 mountain slopes, which has been found to explain daytime CO₂ mixing-ratio decreases at other
 342 mountaintop sites (e.g. Sun et al. 2007). Night-time CO₂ mixing ratios are characterized by an
 343 increase that occurs independently of the daytime maximum PBL height relative to the ridgetop
 344 and can be attributed to, e.g. on-site respiration in the growing season.

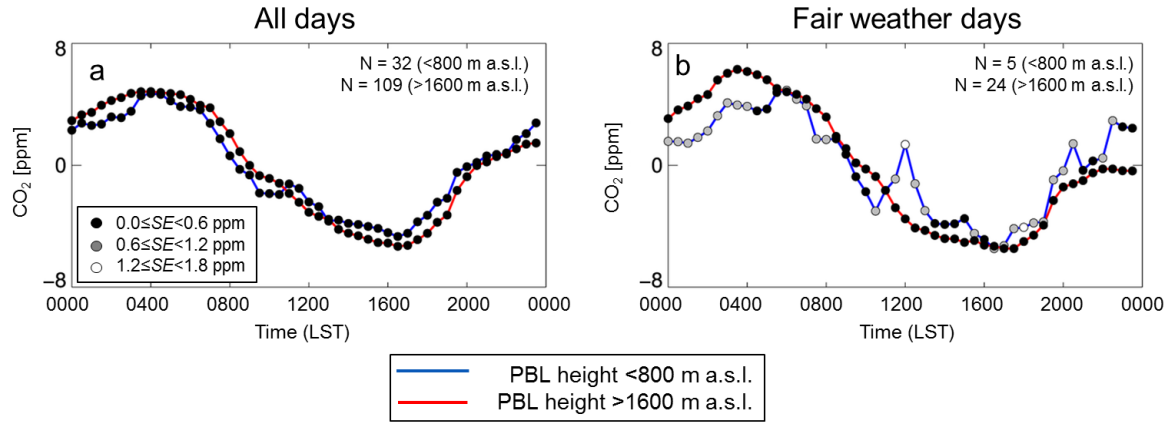


345
 346 **Fig 3** Mean diurnal cycle in CO mixing ratio, measured 17 m a.g.l., for PBL heights <800 m (blue line) and for PBL
 347 heights >1600 m (red line) for all days over the period 1 January 2009 – 31 December 2012 (a) and for the subset of
 348 fair weather days with constant wind directions (b). Same for panels (c) and (d) but for CO₂ mixing ratio measured
 349 17 m a.g.l. at the Pinnacles site. The number of cases of PBL height <800 m a.s.l. and PBL height >1600 m a.s.l., *N*,
 350 is noted in each panel. The circles represent the standard error in the measurements, and the legend for each species
 351 is shown on panels (a) and (c). For brevity, the standard error is shown every 60 min rather than every 30 min.

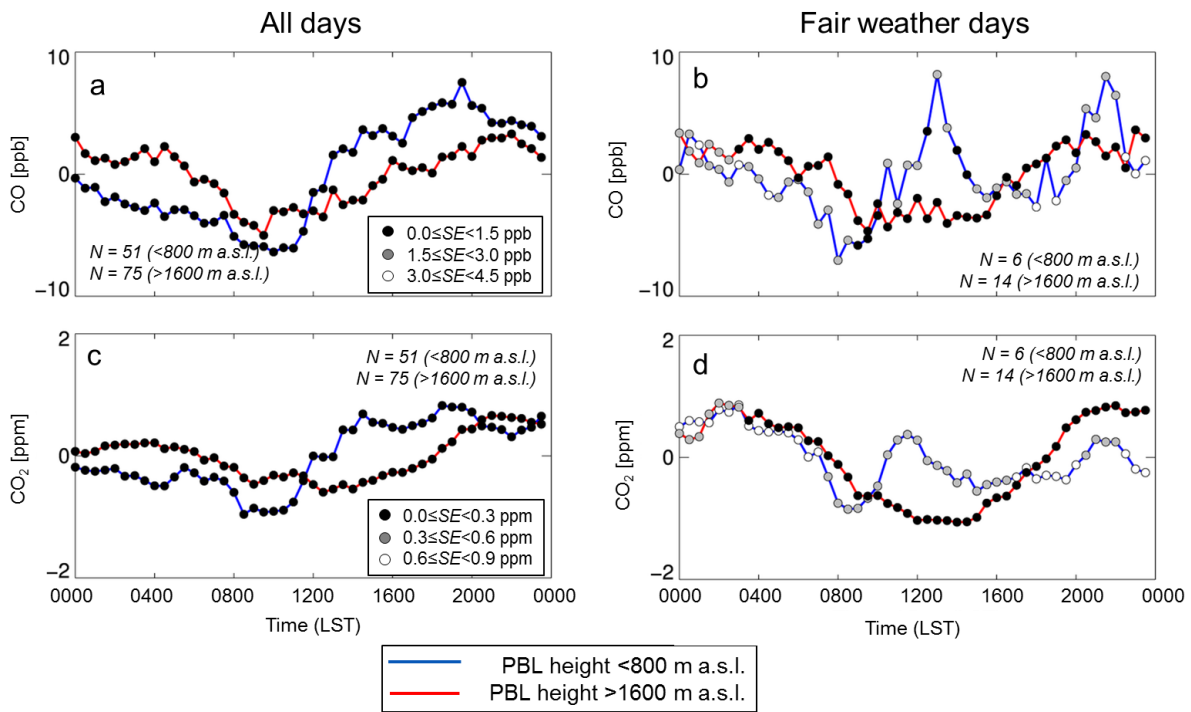
352 4.3.3 Seasonal Differences between CO and CO₂ Mixing-Ratio Diurnal Cycles

353 Because the seasonal cycle of CO₂ mixing ratios is strongly affected by photosynthetic uptake
354 and respiration during the growing season, we differentiated between the mean diurnal cycles in
355 the two contrasting seasons (summer and winter) for the subset of days with PBL heights below
356 the ridgetop and for the subset of days with PBL heights above the ridgetop. We found that the
357 amplitude of the diurnal CO₂ mixing-ratio cycle is largest on fair weather days with PBL heights
358 exceeding the ridgetop height during the summer (Fig. 4), whereas diurnal CO₂ mixing-ratio
359 changes are smallest on days with deep PBL heights during the winter (Fig. 5). Most notable,
360 however, is a daytime CO₂ mixing-ratio increase during the winter when the PBL remains below
361 the ridgetop that begins around 1100 LST and leads to maximum CO₂ mixing ratios around 1800
362 LST (Fig. 5c). A CO₂ mixing-ratio increase is also observed in summer (Fig. 4) but is much less
363 pronounced and shorter-lived than in winter. Regardless of whether the PBL is below the
364 ridgetop or is above the ridgetop, CO and CO₂ mixing ratios closely follow the same cycle during
365 the winter which indicates that, when CO₂ uptake is absent, CO and CO₂ mixing ratios behave as
366 similar tracers of atmospheric dynamics at the site. The similar behaviour of the diurnal CO and
367 CO₂ mixing-ratio cycles during the winter, particularly the daytime CO and CO₂ mixing-ratio
368 increase on days with PBL heights below the mountaintop suggests that they are mainly
369 influenced by polluted air arriving at the mountaintop during the daytime from the adjacent
370 valleys. We hypothesize that its origin can be traced to the upwind adjacent valley; we
371 investigate this hypothesis in more detail in the next section.

372



373
 374 **Fig 4** Diurnal CO₂ mixing-ratio cycle for all days (a) and for the subset of fair weather days with constant winds (b)
 375 for the summer (1 June – 31 August) months. The circles represent the standard error in the measurements.
 376



377
 378 **Fig 5** Same as Fig. 3 but only for days during the winter months (1 December – 28 February).
 379

380 4.4 Indicators of Valley-PBL Air Impacting the Mountaintop Measurements

381 In the previous section, we discussed the [diurnal](#) CO and CO₂ mixing-ratio cycles as a function
382 of PBL height relative to the mountaintop height. These diurnal CO mixing-ratio changes closely
383 follow changes in specific humidity (q) on the subset of fair weather days with constant wind
384 directions for both the subsets of days with PBL heights below the ridgetop and for the subset of
385 days with PBL heights above the ridgetop (Fig. 6b). On days with the PBL height below the
386 ridgetop, the simultaneous CO mixing ratio and specific humidity increases indicate that these
387 days are characterized by vertical transport and mixing of valley-PBL air to the mountaintop
388 (e.g. Weiss-Penzias et al. 2006). Previous studies (i.e. Lee and De Wekker 2016) from the site
389 have found, through the combined use of observations and numerical simulations, that these
390 cases are characterized by a daytime PBL that parallels the underlying terrain. Shallow daytime
391 PBLs that closely parallel the underlying terrain have also been reported in studies involving
392 other mountaintops (e.g. De Wekker 2002; De Wekker and Kossman 2015). The transport of
393 valley-PBL air to the mountaintop within this shallow terrain-following daytime PBL results in a
394 short-lived increase in CO₂ mixing ratio that corresponds with the peak in specific humidity and
395 has been attributed in previous studies at the site to upslope flows (Pal et al. 2017). In contrast,
396 the decrease in passive tracers like specific humidity that accompanies the decrease in CO
397 mixing ratio on days with the PBL height above the ridgetop, as well as the absence of a
398 noontime increase in CO₂ mixing ratio, implies that PBL dilution and entrainment overwhelm
399 the transport of polluted valley-PBL air to the mountaintop via convective mixing and upslope
400 flows.

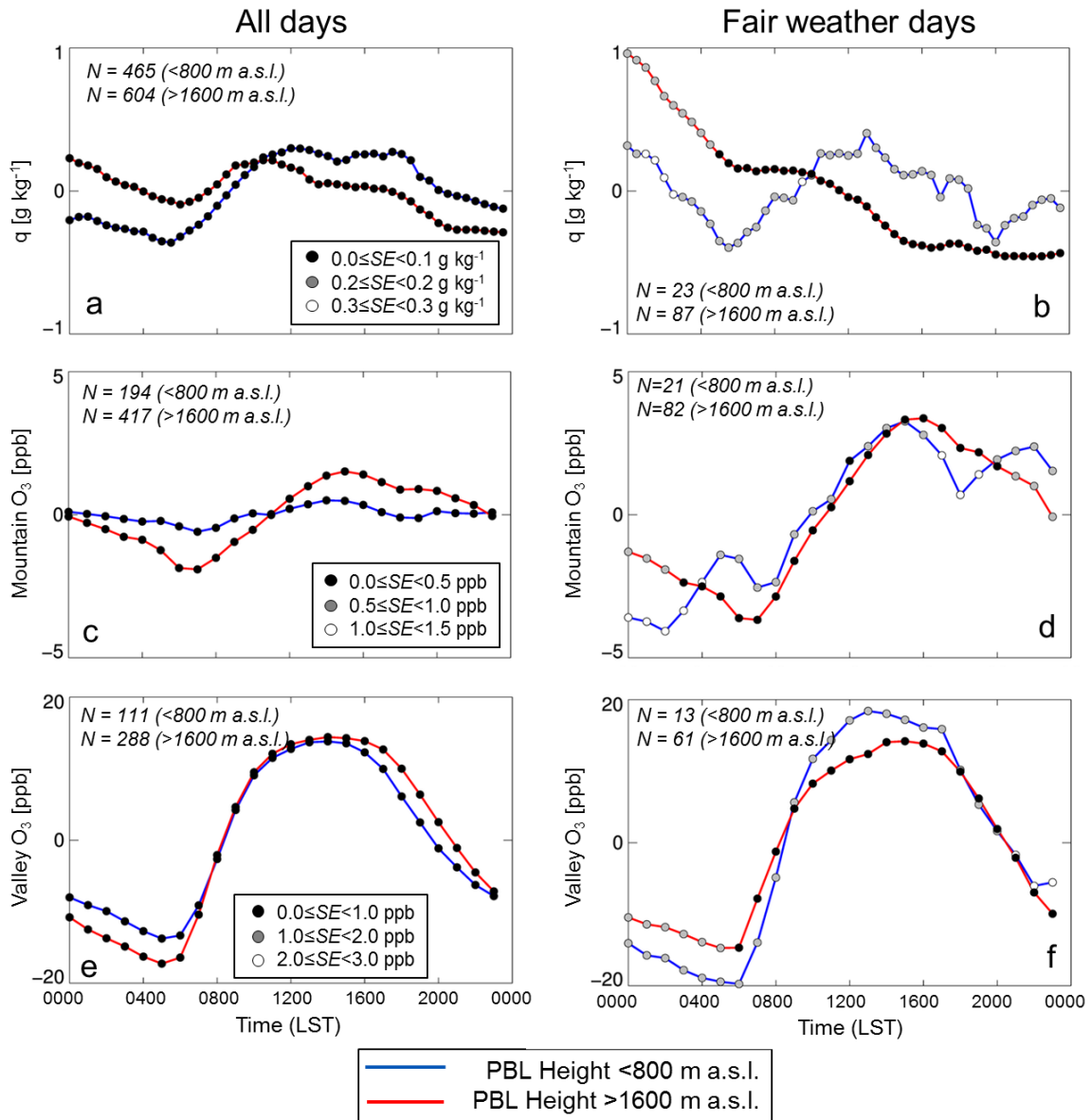
401 The relationships between CO mixing ratio and specific humidity, as well as CO₂ mixing
402 ratio and specific humidity, as a function of PBL height relative to the ridgetop are less clear

403 when all days in the period of record are considered (Fig. 6a). When the PBL height is below the
404 ridgetop, both CO mixing ratios and specific humidity increase beginning around 0700 LST,
405 whereas CO₂ mixing ratios decreases (c.f. Fig. 3c). However, specific humidity remains
406 somewhat constant between 1200 LST and 1900 LST, but during this time CO mixing ratios kept
407 increasing and CO₂ mixing ratios decrease (c.f. Fig. 3a, 3c). On fair weather days with constant
408 wind directions and PBL tops below the ridgetop, CO mixing ratios and specific humidity
409 increase after the onset of stable boundary-layer development around sunset to a secondary
410 maximum around 2300 LST (c.f. Fig. 3b, Fig. 6b). In the case of CO₂ mixing ratio, respiration
411 also contributes to the nocturnal CO₂ mixing-ratio increase.

412 When days with PBL heights above the ridgetop height are considered irrespective of wind-
413 direction shift or the day's clearness index, CO mixing ratio and specific humidity decrease
414 throughout the entire night. However, the **amplitude** of the CO mixing ratio decrease on the
415 subset of fair weather days with constant wind directions is about 4 ppb larger than the mean CO
416 mixing ratio cycle of all days with PBL heights exceeding the ridgetop height. One possible
417 reason for this larger CO mixing ratio decrease is more pronounced nocturnal downslope flows
418 under fair weather conditions (e.g. Zardi and Whiteman, 2013) which result in a transport of
419 clean free atmospheric air to the mountaintop (e.g. Schmidt et al. 1996).

420 O₃ mixing ratios at a nearby mountaintop (at the Big Meadows site, located about 14 km
421 south of the Pinnacles site but at a similar elevation; see Section 2.3) and a valley site also show
422 significant differences in their diurnal cycles that depend on 1) whether or not the day is a fair
423 weather day, and 2) PBL height (Fig. 6c, 6d, 6e, 6f). At the mountaintop, the amplitude in the
424 **diurnal** O₃ mixing-ratio cycle is larger on fair weather days with PBL tops exceeding the ridgetop
425 height (Fig. 6c, 6d). In contrast, the amplitude of the **diurnal** O₃ mixing-ratio cycle at the valley

426 site is largest on fair weather days with PBL tops below the ridgetop (Fig. 6f) due to an increase
 427 in pollutant mixing ratios within a shallow PBL that favors O₃ production. Also note that the
 428 amplitude of the diurnal O₃ mixing-ratio cycle in the valley is much larger than at the
 429 mountaintop (cf. Fig. 6e, 6f and Fig. 6c, 6d).



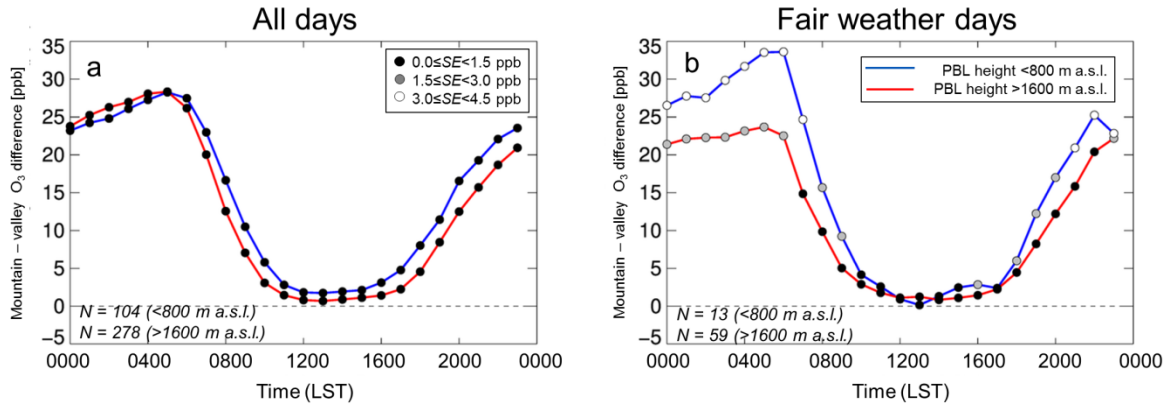
430
 431 **Fig 6** Mean diurnal cycle in specific humidity, measured 17 m a.g.l., for PBL heights <800 m (blue line) and for
 432 PBL heights >1600 m (red line) for all days (a) and for the subset of fair weather days with constant wind directions
 433 (b) independent of season for 1 Jan 2009 – 31 Dec 2012. Panels (c) and (d) show O₃ mixing ratio at the mountaintop

434 (the Big Meadows site), and panels (e) and (f) show O₃ mixing ratio at the valley site (Luray). The number of cases
435 of PBL height <800 m a.s.l. and PBL height >1600 m a.s.l., *N*, is noted in each panel. The circles represent the
436 standard error in the measurements and are shown in the bottom right of panels (a), (c), and (e) for specific
437 humidity, mountaintop O₃ mixing ratios, and valley O₃ mixing ratios, respectively. Note that the daily means are
438 removed.

439

440 The role of valley-PBL air on the mountaintop trace-gas mixing ratios is further investigated
441 by computing the difference in O₃ mixing ratios between the mountaintop and valley. O₃ mixing
442 ratios are 20-30 ppb greater at the mountaintop than in the valley during the night-time (Fig. 7)
443 which has previously been attributed to deposition (e.g. Reitebuch et al. 2000, Mayer et al. 2008)
444 and to enhanced O₃ depletion by nitric oxide in valleys (e.g. Broder and Gygax, 1985, Wunderli
445 and Gehrig, 1990, Vöglin et al. 1996). Additionally, previous studies have shown that the
446 greater nocturnal O₃ mixing ratios at mountaintops occur because the mountaintops are exposed
447 to O₃-rich free atmospheric air via downslope flows (e.g. Zaveri et al. 1995) and elevated O₃
448 layers which oftentimes form over mountainous terrain (e.g. Neu et al. 1994, McKendry and
449 Lundgren 2000). O₃ mixing-ratio differences between the mountaintop and valley become
450 smaller beginning around sunrise and are smallest from about 1000-1700 LST (typically <2 ppb).
451 The small differences are attributed to the mixing of transported valley-PBL air with the air mass
452 at the mountaintop, as reported in previous studies for other mountaintop sites, e.g.
453 Hohenpeissenberg (998 m a.s.l.) (Mayer et al. 2008). We note that these transport processes
454 occur independently of PBL height relative to the mountaintop and independently of the
455 presence of fair weather conditions at the site (Fig. 7b). This finding most likely indicates that
456 valley-PBL air arrives at the mountaintop regardless of the PBL height relative to the

457 mountaintop, and that the mountaintop and valley measure similar trace-gas mixing ratios during
 458 the daytime.

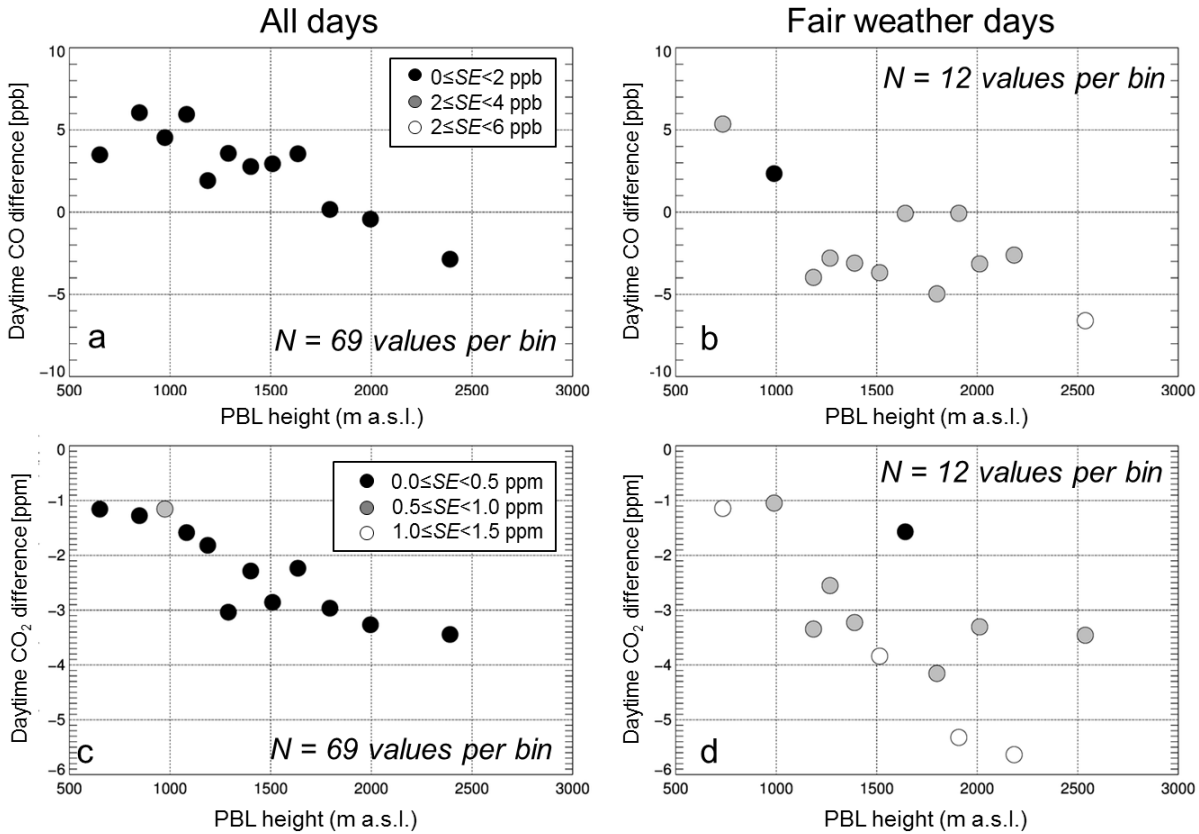


459
 460 **Fig 7** Diurnal cycle in O₃ mixing-ratio difference between the mountaintop and valley for days with PBL heights
 461 <800 m (blue line) and for PBL heights >1600 m (red line) for all days (a) and for the subset of fair weather days
 462 with constant wind directions (b). The circles represent the standard error in the measurements.

463
 464 4.5 Effect of PBL Height on Diurnal Contrasts in CO and CO₂ Mixing Ratios

465 To quantitatively investigate the impacts of PBL dilution and entrainment on the observed
 466 diurnal CO and CO₂ mixing ratios, we could determine the relationship between daily CO and
 467 CO₂ mixing-ratio amplitude and afternoon PBL height. However, the amplitudes represent the
 468 absolute change in CO and CO₂ mixing ratio occurring over the entire diurnal cycle and also
 469 include night-time processes, e.g. nocturnal sinking motions that transport free-atmospheric air to
 470 mountaintops (e.g. Schmidt et al. 1996). These processes can affect the trace-gas cycle
 471 independently of the maximum daytime PBL height. In addition, nocturnal respiration occurring
 472 at local to regional scale can impact the CO₂ mixing-ratio amplitude independently of PBL
 473 height. Therefore, to isolate the impact of processes occurring in the daytime PBL on the diurnal
 474 mountaintop CO and CO₂ mixing-ratio cycle, we computed the difference between mean

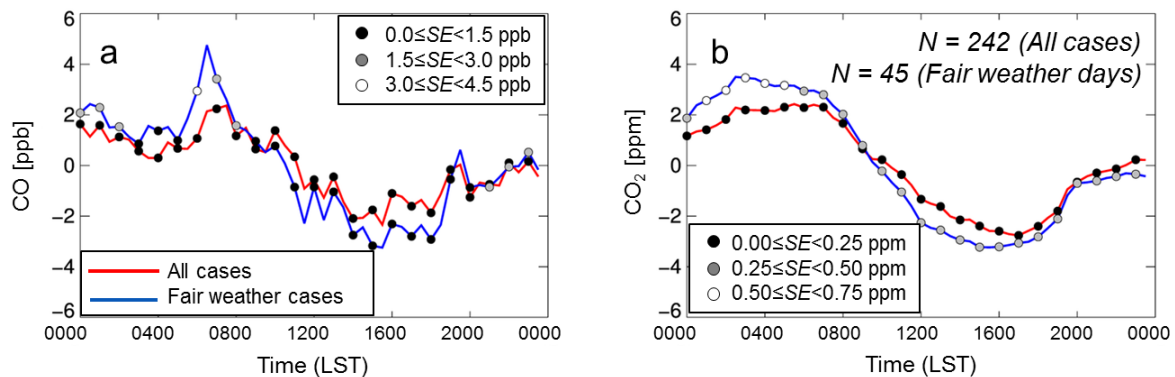
475 afternoon (1200-1600 LST) and mean morning (0400-0800 LST) mixing-ratios rather than the
476 daily amplitudes. There is an inverse relationship between this CO mixing-ratio difference and
477 PBL height when all days are considered ($r = -0.86$, $p < 0.01$) and only when the PBL height
478 exceeds 2000 m a.s.l., CO mixing ratios are typically lower in the afternoon than during the
479 morning (Fig. 8a). On the subset of fair weather days with constant wind directions, there also
480 exists an inverse relationship between PBL height and the daytime CO mixing-ratio difference (r
481 $= -0.67$, $p = 0.02$) (Fig. 8b). Mean CO mixing ratios are about 4 ppb larger during the afternoon
482 than during the morning on days when the PBL height is below the ridgetop because of the
483 upward transport and mixing of pollutants. When the PBL height exceeds the ridgetop, afternoon
484 CO mixing ratios are about 5 ppb lower than morning CO mixing ratios because pollutants are
485 mixed over a volume of air that is larger than on days with a shallow PBL, thereby resulting in a
486 decrease in trace-gas mixing ratios. This decrease is similar to what occurs over flat terrain (e.g.
487 Pochanart et al. 2003, Popa et al. 2010, Pal 2014, Berhanu et al. 2016, Chandra et al. 2016,
488 Sreenivas et al. 2016), and its implications are revisited in Section 5.



489
 490 **Fig 8** Mean difference between mean afternoon (1200-1600 LST) and mean morning (0400-0800 LST) CO mixing
 491 ratios as a function of PBL height for 1 January 2009 – 31 December 2012 for all days (a) and for fair weather days
 492 with constant wind directions (b). Same for panels (c) and (d) but for CO₂ mixing ratio. Data from all days represent
 493 12 bins with 69 values per bin; data from fair weather days represent 12 bins with 11 values per bin.

494
 495 There is also an inverse relationship between the PBL height in the difference between mean
 496 afternoon and mean morning CO₂ mixing ratios ($r = -0.89, p < 0.01$) when either all days are
 497 considered (Fig. 8c) or just the subset of fair weather days ($r = -0.67, p = 0.02$) (Fig. 8d), with a
 498 larger decrease in daytime CO₂ mixing ratio on days with deeper PBLs. The differences between
 499 the morning and afternoon are larger on the subset of fair weather days most likely due to larger
 500 on-site CO₂ fluxes along with deep PBL mixing occurring on days with stronger insolation (not
 501 shown).

502 Both when all days or only fair weather days with constant wind directions are considered,
 503 CO mixing ratios are lower in the afternoon than in the morning on days when the PBL height
 504 greatly exceeds the ridgetop height, i.e. is about 1 km above the ridgetop or at least 2000 m a.s.l.
 505 (Fig. 9a). The mean diurnal CO mixing-ratio cycle in both of these scenarios is characterized by
 506 a CO mixing-ratio maximum around 0730 LST, whereas the minimum CO mixing ratios occur
 507 around 1500 LST in both mean diurnal cycles (Fig. 9a). The decrease in the diurnal CO and CO₂
 508 mixing-ratio cycles (Fig. 9b) both on all days and on the subset of fair weather days suggests the
 509 influences of PBL dilution and entrainment.



510
 511 **Fig 9** Diurnal CO (a) and CO₂ (b) mixing-ratio cycle on all days over the period 1 January 2009 – 31 December
 512 2012 when PBL heights >2000 m a.s.l. (red line, N=242) and for the subset of fair weather days with PBL heights
 513 >2000 m a.s.l. and constant wind directions (blue line, N=45). The circles represent the standard error in the
 514 measurements. For readability, the standard error is shown every 60 min rather than every 30 min.

515

516 5 A Conceptual Framework Highlighting the Key Findings

517 We summarize our findings using a conceptual framework shown in Fig. 10 to illustrate the
 518 dominant physical processes affecting the diurnal cycle of trace gases, specifically CO mixing
 519 ratio, at mountaintops as a function of afternoon valley-PBL top relative to ridgetop height. In
 520 the conceptual diagram, we assume that the valley is the sole source of pollutants. We also

521 assume that there are no chemical reactions, including photosynthetic uptake of CO₂ mixing ratio
522 during summer, that either add or remove the trace gas from the atmosphere, and we neglect
523 surface deposition. Therefore, the conceptual diagram that we present closely matches the
524 diurnal CO mixing-ratio cycles shown in Figs. 3 and 9.

525 On days when the valley-PBL top remains below the ridgetop (Fig. 10a), pollutant transport
526 from the valley to the mountaintop occurs via upslope flows and PBL mixing within a daytime
527 PBL. The result is that pollutants are confined within this shallow PBL that parallels the
528 underlying terrain throughout the day, as shown by the PBL tops during the mid-morning and
529 mid-afternoon in Fig. 10a which correspond with times $t1$ and $t2$, respectively. Between time $t1$
530 and $t2$, pollutants are transported to the mountaintop which causes their mixing ratios at the
531 mountaintop to increase (Fig. 10b). After time $t2$, local mixing occurring with the PBL at the
532 ridgetop causes the pollutant mixing-ratios to decrease. The daytime increase occurs between
533 times $t1$ and $t2$ is contrary to many previous studies that have reported little to no change in
534 daytime trace-gas mixing ratios when the valley PBL remains below the ridgetop height (e.g.
535 Forrer et al. 2000, Obrist et al. 2008, MacDonald et al. 2011).

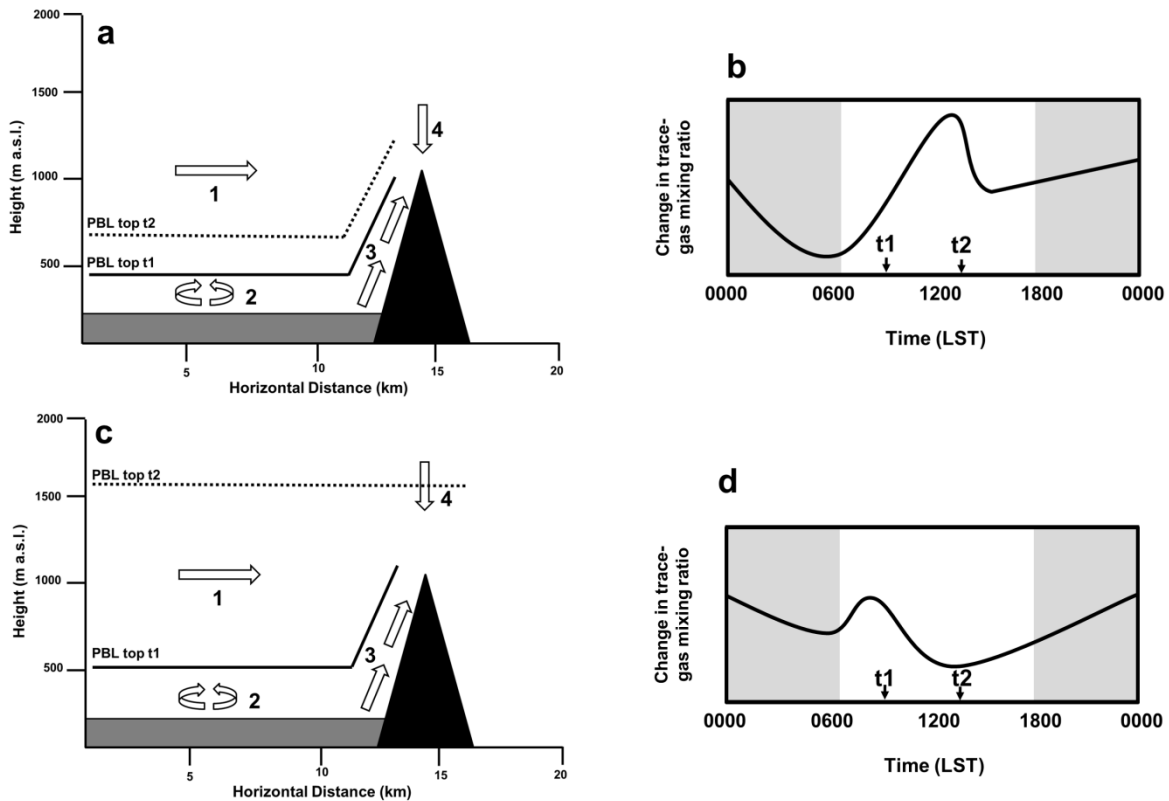
536 A key difference between these previous findings from other mountaintops and our findings
537 is that the previous studies were conducted using measurements from mountaintops with much
538 greater topographic relief than the Pinnacles site, i.e. those that are typically at least 2-3 km in
539 elevation and at least 1-2 km above the surrounding valley or plain (e.g. Keeling et al. 1976,
540 Forrer et al. 2000, De Wekker et al. 2009, McClure et al. 2016, Zhu et al. 2016). Mountaintops
541 with these topographic characteristics remain in the free atmosphere much of the time and are
542 much more isolated from the effects of valley-PBL air because the maximum height of the valley
543 PBL is at least several hundred metres below the ridgetop height. The Pinnacles site is affected

544 by valley-PBL air much more frequently than taller mountaintops as the PBL height is at least
545 500 m over the ridgetop on about one-third of all days. Because of the daytime trace-gas increase
546 that we observe at the Pinnacles site on days with PBL heights below the ridgetop, the daytime
547 trace-gas measurements from the Pinnacles site, as well as other mountaintops with similar
548 elevation above the surrounding valley and where the daytime maximum PBL height does not
549 exceed the ridges, cannot be considered representative of free atmospheric values, but rather are
550 representative of the local valley PBL. Therefore, these measurements should not be assimilated
551 into e.g. inverse carbon transport models or air chemistry models that cannot resolve local to
552 mesoscale processes.

553 On days when valley-PBL heights exceed the ridgetop (i.e. >1600 m a.s.l.) (Fig. 10c), the
554 PBL is initially parallel to the underlying terrain during the mid-morning, as shown by the PBL
555 top at time $t1$ in Figure 10c, like it is on days with PBL heights below the ridgetop. Pollutants are
556 transported to the mountaintop during this time as evident by the short-lived maximum in CO
557 mixing ratios. As the PBL grows deeper during the day and exceeds the ridgetop height, it does
558 not parallel the underlying terrain, as shown by the PBL top at time $t2$. After the mid-morning
559 maximum in pollutant mixing-ratios at time $t1$, we infer that pollutant transport via upslope
560 flows becomes overwhelmed by PBL dilution and the entrainment of cleaner free atmospheric
561 air on these days. Thus, mountaintop pollutant mixing ratios decrease between times $t1$ and $t2$ to
562 an afternoon minimum on these days (Fig. 10d). [This daytime trace-gas mixing ratio decrease is](#)
563 [also contrary to findings from other mountaintops. The key difference between the Pinnacles site](#)
564 [and other mountaintops is that other mountaintops where studies have been conducted are higher](#)
565 [in elevation and extend higher above the surrounding valley/plain than the Pinnacles site \(e.g.](#)
566 [Forrer et al. 2000, Bukowiecki et al. 2016, McClure et al. 2016, Zhu et al. 2016\).](#) At

567 mountaintops with these topographic characteristics, the valley PBL may reach the mountaintop
568 during the daytime but the PBL is not deep enough above the ridgetop for mixing to dilute the
569 pollutants and cause their mixing ratios to decrease.

570 We also note that the daytime pollutant mixing-ratio decrease at the Pinnacles site on days
571 with PBL heights exceeding the ridgetop height is similar to the findings from tall towers in flat
572 terrain (e.g. Schmidt et al. 2014, Pal et al. 2015, Berhanu et al. 2016). Our results on the deep
573 PBL exceeding the ridgetop suggest that, although pollutants arrive at the mountaintop via
574 upslope flows, the impact of these flows on the mountaintop measurements is overwhelmed by
575 PBL dilution and entrainment of free atmospheric air. This same process occurs in flat terrain,
576 where PBL dilution and entrainment cause a decrease in pollutant mixing ratios, and suggests
577 that low-elevation mountaintops such as the Pinnacles site behave like tall towers. The same is
578 also true for other mountaintops where the regional PBL exceeds the ridgetop height. Based on
579 these findings, selecting days on which PBL heights over the adjacent valley or plains exceed the
580 mountaintop height can be used as guidance for identifying trace-gas measurements
581 representative of the regional PBL. Trace-gas measurements made during the afternoon on these
582 days can then be used for assimilation into regional scale inverse carbon transport models and air
583 chemistry studies.



584

585 **Fig 10** Conceptual diagram of dominant trace-gas transport mechanisms, assuming the valley (grey rectangle) is the
 586 sole source of pollutants, affecting the diurnal cycle of a passive trace gas as a function of PBL height relative to a
 587 1000 m a.s.l. mountaintop (black triangle) on days when the height of the afternoon valley PBL remains below the
 588 mountaintop. The dominant transport mechanisms shown are synoptic-scale advection (1), convective mixing (2),
 589 upslope flows (3), and free atmosphere air entrainment (4) and are indicated with arrows. The PBL top at times $t1$
 590 and $t2$ is shown by solid and dotted lines, respectively. These times are indicated on panel (b) which shows the near-
 591 surface diurnal trace-gas cycle starting with a set mixing ratio of trace gas and assuming no advection or sources.
 592 The shaded and non-shaded areas in this panel represent night-time and daytime, respectively. Same for panels (c)
 593 and (d) but for days when PBL height is much greater than the height of the mountaintop.

594

595 6 Summary and Conclusions

596 We presented the first study investigating the effect of the afternoon PBL height on the diurnal
 597 CO and CO₂ mixing-ratio cycle at a low mountaintop using measurements from a mountaintop

598 trace-gas monitoring site (the Pinnacles site, in the Virginia Blue Ridge Mountains). We found
599 that the diurnal cycle of CO mixing ratios is typically largest on days when the PBL height
600 remained below the ridgetop (i.e., ≈ 1000 m a.s.l.) and is smallest on days when the PBL height
601 exceeded the ridgetop by at least 400 m. On days when the valley-PBL height is below the
602 ridgetop, there is a daytime CO mixing-ratio increase, as well as a short-lived increase in CO₂
603 mixing ratios during the winter, caused by the transport of polluted valley-PBL air to the
604 mountaintop. On days when the valley-PBL height exceeds the ridgetop height, both CO and
605 CO₂ mixing ratio decrease during the daytime due to dilution and entrainment that negate the
606 influence of pollutant transport from the valley floor.

607 The results in this study provide additional insights into the use of trace-gas measurements
608 from low-elevation mountaintops like the Pinnacles site in applications requiring regionally-
609 representative values. The present study builds upon previous studies from the region (Lee et al.
610 2012, 2015, Pal et al. 2017) by helping to further understand the local scale to mesoscale
611 meteorological processes affecting the trace-gas cycle at low mountaintops. The daytime CO
612 mixing-ratio increase on days with PBL heights below the ridgetop, as well as the small
613 differences in O₃ mixing ratio between the mountaintop and valley, suggest that the mountaintop
614 is mostly influenced by valley-PBL air, and therefore the mountaintop trace-gas measurements
615 are representative of the “local” valley atmosphere. Pollutants are also transported to the
616 mountaintop during the daytime on days when the PBL exceeds the ridgetop height, but PBL
617 dilution overwhelms the influence of upslope pollutant transport, causing CO and CO₂ mixing
618 ratios to decrease. This behaviour in CO and CO₂ mixing ratios is also observed in measurements
619 from tall towers (i.e. larger than a few hundred metres a.g.l., or more than about 10% of the
620 daytime PBL depth) in flat terrain. The daytime decrease that we observed indicates that

621 afternoon trace-gas measurements from low mountaintops made when PBL heights over the
622 adjacent valley or plains exceed the ridgetop can be used in the same way that afternoon
623 measurements from tall towers are used in applications requiring regionally-representative
624 measurements.

625

626 **7 Tables**

Season	Correction (m)
Winter	+190
Spring	+210
Summer	+300
Fall	+250

627 **Table 1** Seasonal correction factor applied to the Dulles Airport rawinsonde PBL height, based on findings from
628 Lee and De Wekker (2016), to better approximate the daytime maximum PBL height over the Page Valley.

629

630 **Acknowledgements** This research and maintenance of the Pinnacles site was partly funded by an MOU between the
631 NOAA Earth System Research Laboratory (ESRL) Global Monitoring Division, by NOAA award
632 NA13OAR4310065, and by NSF-CAREER award ATM-1151445. We thank Željko Večenaj at the University of
633 Zagreb for advice on instrument maintenance. We acknowledge Arlyn Andrews at NOAA ESRL as the primary
634 provider of the CO mixing-ratio data, and Jonathan Kofler and Jonathan Williams at NOAA ESRL who assisted
635 with the installation and maintenance of the CO and CO₂ mixing-ratio monitoring system. We also thank staff from
636 Shenandoah National Park, especially Elizabeth Garcia, Jim Schaberl, and Alan Williams, as well as Nevio Babić,
637 Stephanie Phelps, and Mark Sghiatti from the University of Virginia Environmental Sciences Department for
638 helping maintain data collection at the Pinnacles site. The CO and CO₂ mixing-ratio datasets used are accessible for
639 public research through NOAA ESRL (ftp://aftp.cmdl.noaa.gov/data/trace_gases/co/in-situ/tower/snp/). Finally, we
640 thank the two anonymous reviewers whose suggestions helped improve the quality of the paper.

641

642 **References**

- 643 Andrews AE, Kofler JD, Trudeau ME, Williams JC, Neff DH, Masarie KA, Chao DY, Kitzis DR, Novelli PC, Zhao
644 CL, Dlugokencky EJ, Lang PM, Crotwell MJ, Fischer ML, Parker MJ, Lee JT, Baumann DD, Desai AR,
645 Stanier CO, De Wekker SFJ, Wolf DE, Munger JW, Tans PP (2014) CO₂, CO, and CH₄ measurements
646 from tall towers in the NOAA Earth System Research Laboratory's Global Greenhouse Gas Reference
647 Network: instrumentation, uncertainty analysis, and recommendations for future high-accuracy greenhouse
648 gas monitoring efforts. *Atmos Meas Tech* 7:647–687
- 649 Atlas EL, Ridley BA (1996) The Mauna Loa Observatory photochemistry experiment: introduction. *J Geophys Res*
650 101(D9):14531–14541
- 651 Baltensperger U, Gäggeler HW, Jost DT, Lugauer M, Schwikowski M, Weingartner E (1997) Aerosol climatology
652 at the high-alpine site Jungfraujoch, Switzerland. *J Geophys Res* 102(D16):19707-19715
- 653 Balzani Lööv JM, Henne S, Legreid G, Staehelin J, Reimann S, Prévôt ASH, Steinbacher M, Vollmer MK (2008)
654 Estimation of background concentrations of trace-gases at the Swiss alpine site Jungfraujoch (3580 m asl).
655 *J Geophys Res* 113(D22305)
- 656 Bamberger I, Oney B, Brunner D, Henne S, Leuenberger M, Buchmann N, Eugster W (2017) Observations of
657 atmospheric methane and carbon dioxide mixing-ratios: tall-tower or mountaintop stations? *Boundary-*
658 *Layer Meteorol.* doi:10.1007/s10546-017-0236-3.
- 659 Berhanu TA, Satar E, Schanda R, Nyfeler P, Moret H, Brunner D, Oney B, Leuenberger M (2016) Measurements of
660 greenhouse gases at Beromünster tall-tower station in Switzerland. *Atmos Meas Tech* 9:2603-2614
- 661 Broder B, Gygax HA (1985) The influence of locally induced wind systems on the effectiveness of nocturnal dry
662 deposition of ozone. *Atmos Environ* 19:1627–1637
- 663 Brooks BJ, Desai AR, Stephens BB, Bowling DR, Burns SP, Watt AS, Heck SL, Sweeney C (2012) Assessing
664 filtering of mountaintop CO₂ mole fractions for application to inverse models of biosphere-atmosphere
665 carbon exchange. *Atmos Chem Phys* 12:2099–2115
- 666 Bukowiecki N, Weingartner E, Gysel M, Collaud Coen M, Zieger P, Herrmann E, Steinbacher M, Gäggeler HW,
667 Baltensperger U (2016) A review of more than 20 years of aerosol observation at the high altitude Research
668 station Jungfraujoch, Switzerland (3580 m asl). *Aerosol Air Qual Res* 16:764–788.

669 Chandra N, Lal S, Venkataramani S, Patra PK, Sheel V (2016) Temporal variations of atmospheric CO₂ and CO at
670 Ahmedabad in western India. *Atmos Chem Phys*. 16:6153–6173

671 Cristofanelli P, Fierli F, Marinoni A, Calzolari F, Duchi R, Burkhardt J, Stohl A, Maione M, Arduini J, Bonasoni P
672 (2013) Influence of biomass burning and anthropogenic emissions on ozone, carbon monoxide and black
673 carbon at the Mt. Cimone GAW-WMO global station (Italy, 2165 m asl). *Atmos Chem Phys* 13:15–30

674 Dabberdt WF, Carroll MA, Baumgardner D, Carmichael G, Cohen R, Dye T, Ellis J, Grell G, Grimmond S, Hanna
675 S, Irwin J, Lamb B, Madronich S, McQueen J, Meagher J, Odman T, Pleim J, Schmid HP, Westphal DL
676 (2004) Meteorological research needs for improved air quality forecasting: Report of the 11th prospectus
677 development team of the U.S. Weather Research Program. *B Amer Meteorol Soc* 85:563–586

678 De Wekker SFJ, Zhong S, Fast JD, Whiteman CD (1998) A numerical study of the thermally driven plain-to-basin
679 wind over idealized basin topographies. *J Appl Meteorol* 37:606–622

680 De Wekker, SFJ (2002) Structure and morphology of the convective boundary layer in mountainous Terrain. Ph.D.
681 Dissertation, The University of British Columbia, BC, Canada, 191 pp.

682 De Wekker SFJ, Steyn DG, Nyeki S (2004) A comparison of aerosol-layer and convective boundary-layer structure
683 over a mountain range during STAARTE '97. *Bound-Lay Meteorol* 113(2):249–271

684 De Wekker SFJ, Ameen A, Song G, Stephens BB, Hallar AG, McCubbin IB (2009) A preliminary investigation of
685 boundary layer effects on daytime atmospheric CO₂ concentrations at a mountaintop location in the Rocky
686 Mountains. *Acta Geophys* 57(4):904–922

687 De Wekker SFJ, Kossmann M (2015) Convective boundary layer heights over mountainous terrain – A review of
688 concepts. *Front Earth Sci* 3(77)

689 Elanky NF, Lokoshchenko MA, Belikov IB, Skorokhod AI, Shumskii RA (2007) Variability of trace-gases in the
690 atmospheric boundary layer from observations in the city of Moscow. *Atmos Ocean Phys* 43(2):219–231

691 Forrer J, Rüttiman R, Schneiter D, Fischer A, Buchmann B, Hofer P (2000) Variability of trace-gases at the high-
692 Alpine site Jungfrauoch caused by meteorological transport processes. *J Geophys Res* 105(D10):12241–
693 12251

694 Gao J, Wang T, Ding A, Liu C (2005) Observational study of ozone and carbon monoxide at the summit of mount
695 Tai (1534 m asl) in central-eastern China. *Atmos Environ* 39:4779–4991

696 Gibert F, Schmidt M, Cuesta J, Ciais P, Ramonet M, Xueref I, Larmanou E, Flamant PH (2007) Retrieval of average
697 CO₂ fluxes by combining in situ CO₂ measurements and backscatter lidar information. *J Geophys Res*
698 112(D10301)

699 Greco S, Baldocchi DD (1996) Seasonal variations of CO₂ and water vapour exchange rates over a temperate
700 deciduous forest. *Global Change Biol* 2:183–197

701 Henne S, Dommen J, Neininger B, Reimann S, Staehelin J, Prévôt ASH (2005) Influence of mountain venting in the
702 Alps on the ozone chemistry of the lower free troposphere and the European pollution export. *J Geophys*
703 *Res* 110(D22307)

704 Henne S, Junkermann W, Kariuki JM, Aseyo J, Klausen J (2008a) Mount Kenya Global Atmospheric Watch Station
705 (MKN): Installation and meteorological characterization. *J Appl Meteorol Clim* 47:2946–2962

706 Henne S, Klausen J, Junkermann W, Kariuki JM, Aseyo JO, Buchmann B (2008b) Representativeness and
707 climatology of carbon monoxide and ozone at the global GAW station Mt. Kenya in equatorial Africa.
708 *Atmos Chem Phys* 8:3119–3139

709 Hondula DM, Davis RE, Knight DB, Sitka LJ, Enfield K, Gawtry SB, Stenger PJ, Deaton ML, Normile CP, Lee TR
710 (2013) A respiratory alert model for the Shenandoah Valley, Virginia, USA. *Int J Biometeorol* 57:91–105

711 Keeling CD, Bacastow RB, Bainbridge AE, Ekdahl CA, Guenther PR, Waterman LS, Chin JFS (1976) Atmospheric
712 carbon-dioxide variations at Mauna-Loa Observatory, Hawaii. *Tellus* 28(6):538–551

713 Koffi EN, Bergamaschi P, Karstens U, Krol M, Segers A, Schmidt M, Levin I, Vermeulen AT, Fisher RE, Kazan V,
714 Klein Baltink H, Lowry D, Manca G, Meijer HAJ, Moncrieff J, Pal S, Ramonet M, Scheeren HA (2016)
715 Evaluation of the boundary layer dynamics of the TM5 model over Europe. *Geosci Model Dev* 9:3137–
716 3160

717 Lee TR, De Wekker SFJ, Andrews AE, Kofler J, Williams J (2012) Carbon dioxide variability during cold front
718 passages and fair weather days at a forested mountaintop site. *Atmos Environ* 46:405–416

719 Lee TR, De Wekker SFJ, Wofford JEB (2014) Downscaling maximum temperature projections to subkilometer
720 resolutions in the Shenandoah National Park of Virginia, USA. *Adv Meteorol* 2014

721 Lee TR (2015) The impact of planetary boundary layer dynamics on mountaintop trace-gas variability. PhD
722 dissertation, University of Virginia, pp 213

723 Lee TR, De Wekker SFJ, Pal S, Andrews AE, Kofler J (2015) Meteorological controls on the diurnal variability of
724 carbon monoxide mixing-ratio at a mountaintop monitoring site in the Appalachian Mountains. *Tellus B*
725 67(25659)

726 Lee TR, De Wekker SFJ (2016) Estimating daytime planetary boundary layer heights over a valley from rawinsonde
727 observations at a nearby airport: An application to the Page Valley in Virginia, USA. *J Appl Meteor*
728 *Climatol* 55(3):791–809

729 Lee TR, Pal S (2017) On the potential of 25 years (1991–2015) of rawinsonde measurements for elucidating
730 climatological and spatiotemporal patterns of afternoon boundary layer depths over the contiguous US.
731 *Adv Meteorol* 2017:6841239

732 Lin JC, Mallia DV, Wu D, Stephens BB (2017) How can mountaintop CO₂ observations be used to constrain
733 regional carbon fluxes? *Atmos. Chem. Phys.*, 17, 5561–5581.

734 Lin YC, Lin CY, Lin PH, Engling G, Lan Y, Kuo T, Hsu WT, Ting C (2011) Observations of ozone and carbon
735 monoxide at Mei-Feng mountain site (2269 m asl) in Central Taiwan: seasonal variations and influence of
736 Asian continental outflow. *Sci Total Environ* 409:3033–3042

737 Lugauer M, Baltensperger U, Furger M, Gäggeler HW, Jost DT (1998) Aerosol transport to the high Alpine sites
738 Jungfraujoch (3454 m asl) and Colle Gnifetti (4452 m asl). *Tellus B* 50:76–92

739 MacDonald AM, Anlauf KG, Leaitch WR, Chan E, Tarasick DW (2011) Interannual variability of ozone and carbon
740 monoxide at the Whistler high elevation site: 2002–2006. *Atmos Chem Phys* 11:11431–11446

741 Mayer J-C, Staudt K, Gilge S, Meixner FX, Foken T (2008) The impact of free convection on late morning ozone
742 decreases on an Alpine foreland mountain summit. *Atmos Chem Phys* 8:5941–5956

743 Mesinger F, DiMego G, Kalnay E, Mitchell K, Sharfran PC, Ebisuzaki WE, Jović D, Woollen J, Rogers E, Berbery
744 EH, Ek MB, Fan Y, Grumbine R, Higgins W, Li H, Lin Y, Manikin G, Parrish D, Shi W (2006) North
745 American Regional Reanalysis. *Bull Amer Meteor Soc* 87:343–360.

746 McClure CD, Jaffe DA, Gao H (2016) Carbon dioxide in the free troposphere and boundary layer at the Mt.
747 Bachelor Observatory. *Aerosol Air Qual Res* 16:717-728.

748 McKendry IG, Lundgren J (2000) Tropospheric layering of ozone in regions of urbanized complex and/or coastal
749 terrain: a review. *Prog Phys Geog* 24:329–354

750 Neu, U, Künzle T, Wanner H (1994) On the relation between ozone storage in the residual layer and daily variation
751 in near-surface ozone concentration — A case study. *Bound-Layer Meteor* 69(3):221–247

752 Novelli PC, Masarie KA, Lang PM (1998) Distributions and recent changes of carbon monoxide in the lower
753 troposphere *J Geophys Res* 103(D15):19015–19033

754 Obrist D, Hallar AG, McCubbin I, Stephens BB, Rahn T (2008) Measurements of atmospheric mercury at Storm
755 Peak Laboratory in the Rocky Mountains: Evidence for long-range transport from Asia, boundary layer
756 contributions, and plant mercury uptake. *Atmos Environ* 42:7579–7589

757 Ou-Yang C, Lin N, Sheu G, Lee C, Wang J (2014) Characteristics of atmospheric carbon monoxide at a high-
758 mountain background station in East Asia. *Atmos Environ* 89:613–622

759 Pal S (2014) Monitoring depth of shallow atmospheric boundary layer to complement LiDAR measurements
760 affected by partial overlap. *Rem Sens* 6(9):8468–8493

761 Pal S, Lee TR, Phelps S, De Wekker SFJ (2014) Impact of atmospheric boundary layer depth variability and wind
762 reversal on the diurnal variability of aerosol concentration at a valley site. *Sci Total Environ* 496:424–434

763 Pal S, Lopez M, Schmidt M, Ramonet M, Gibert F, Xueref-Remy I, Ciais P (2015) Investigation of the atmospheric
764 boundary layer depth variability and its impact on the ²²²Rn concentration at a rural site in France. *J*
765 *Geophys Res Atmos* 120(2):623–643.

766 Pal S, De Wekker SFJ, Emmitt GD (2016) Spatial variability of the atmospheric boundary layer heights over a low
767 mountain region: Cases from MATERHORN-2012 field experiment. *J Appl Meteor Climatol* 55(9):1927–
768 1952

769 Pal S, Lee TR, De Wekker SFJ (2017) Combined impact of boundary layer height and near-surface meteorological
770 conditions on the CO diurnal cycle at a low mountaintop site: Case studies using simultaneous lidar and in-
771 situ observations. *Atmos Environ* 164, 165-179.

772 Peters W, Jacobson AR, Sweeney C, Andrews AE, Conway TJ, Masarie K, Miller JB, Bruhwiler LMP, Pétron G,
773 Hirsch AI, Worthy DEJ, van der Werf GR, Randerson JT, Wennberg PO, Krol MC, Tans PP (2007) An
774 atmospheric perspective on North American carbon dioxide exchange: CarbonTracker. *P Natl Acad Sci*
775 104(48):18925–18930

776 Peters W, Krol MC, van der Werf GR, Houweling S, Jones CD, Hughes J, Schaefer K, Masarie KA, Jacobson AR,
777 Miller JB, Cho CH, Ramonet M, Schmidt M, Ciattaglia L, Apadula F, Heltai D, Meinhardt F, di Sarra AG,

778 Piacentino S, Sferlazzo D, Aalto T, Hatakka J, Ström J, Haszpra L, Meijer HAJ, van der Laan S, Neubert,
779 REM, Jordan A, Rodo X, Morguí J, Vermeulen AT, Popa E, Rozanski K, Zimnoch M, Manning AC,
780 Leuenberger M, Uglietti C, Dolman AJ, Ciais P, Heimann M, Tans PP (2010) Seven years of recent
781 European net terrestrial carbon dioxide exchange constrained by atmospheric observations. *Glob Change*
782 *Biol* 16:1317–1337

783 Pillai D, Gerbig C, Ahmadov R, Rodenbeck C, Kretschmer R, Koch T, Thompson R, Neiningen B, Lavrie JV (2011)
784 High-resolution simulations of atmospheric CO₂ over complex terrain representing the Ochsenkopf
785 mountain tall tower. *Atmos Chem Phys* 11:7445–7464

786 Pochanart P, Akimoto H, Kajii Y, Sukasem P (2003) Carbon monoxide, regional-scale transport, and biomass
787 burning in tropical continental Southeast Asia: Observations in rural Thailand. *J Geophys Res*
788 108(D17):4552

789 Popa ME, Gloor M, Manning AC, Jordan A, Schultz U, Haensel F, Seifert T, Heimann M (2010) Measurements of
790 greenhouse gases and related tracers at Bialystok tall tower station in Poland. *Atmos Meas Tech* 3:407–427

791 Reitebuch O, Strassburger A, Emeis S, Kuttler W (2000) Nocturnal secondary ozone concentration maxima
792 analyzed by sodar observations and surface measurements. *Atmos Environ* 34:4315–4329

793 Rotach MW, Zardi D (2007) On the boundary-layer structure over highly complex terrain: Key findings from MAP.
794 *Q J Roy Meteor Soc* 133:937–948

795 Schmidt M, Graul R, Sartorius H, Levin I (1996) Carbon dioxide and methane in continental Europe: a climatology,
796 and ²²²Radon-based emission estimates. *Tellus* 48B, 457–473

797 Schmidt M, Graul R, Sartorius H, Levin I (2003) The Schauinsland CO₂ record: 30 years of continental observations
798 and their implications for the variability of the European CO₂ budget. *J Geophys Res* 108(D19):4619

799 Schmidt M, Lopez, M, Kwok CY, Messenger C, Ramonet M, Wastine B, Vuillemin C, Truong F, Gal B, Parmentier
800 E, Cloué O, Ciais P (2014) High-precision quasi-continuous atmospheric greenhouse gas measurements at
801 Trainou tower (Orléans forest, France). *Atmos Meas Tech* 7:2283–2296

802 Seinfeld JH, Pandis SN (1999) Atmospheric chemistry and physics: from air pollution to climate change. John
803 Wiley, New York, New York, 1120 pp

804 Sreenivas S, Mahesh P, Subin J, Kanchana AL, Rao PVN, Dadhwal VK (2016) Influence of meteorology and
805 interrelationship with greenhouse gases (CO₂ and CH₄) at a suburban site of India. *Atmos Chem Phys*
806 16:3953–3967

807 Steyn DG, De Wekker SFJ, Kossmann M, Martilli A (2013) Boundary layers and air quality in mountainous terrain.
808 In: Chow FK, De Wekker SFJ, Snyder BJ (eds) *Mountain weather research and forecasting. Recent*
809 *progress and current challenges*, Springer, Berlin, pp 261–290

810 Stull RB (1988) *An introduction to boundary layer meteorology*. Kluwer Academic Publishers, Dordrecht, pp 670

811 Sullivan, JT, McGee TJ, Langford AO, Alvarez RJ, Senff CJ, Reddy PJ, Thompson AM, Twigg LW, Sumnicht GK,
812 Lee P, Weinheimer A, Knote C, Long RW, Hoff RM (2016) Quantifying the contribution of thermally
813 driven recirculation to a high-ozone event along the Colorado Front Range using lidar. *J. Geophys. Res.*
814 *Atmos.* 121:10377–10390.

815 Sun J, Burns SP, Delany AC, Oncley SP, Turnipseed AA, Stephens BB, Lenschow DH, LeMone MA, Monson RK,
816 Anderson DE (2007) CO₂ transport over complex terrain. *Agricult Forest Meteorol* 145:1–21

817 Thompson AM (1992) The oxidizing capacity of the earth's atmosphere: probable past and future changes. *Science*
818 256(5060):1157–1165

819 Thoning KW, Tans PP, Komhyr WD (1989) Atmospheric carbon dioxide at Mauna Loa Observatory. 2: Analysis of
820 the NOAA/GMCC data, 1974-1985. *J Geophys Res* 94:8549–8565

821 van der Molen MK, Dolman AJ (2007) Regional carbon fluxes and the effect of topography on the variability of
822 atmospheric CO₂. *J Geophys Res Atmos* 112(D01104)

823 Vogelezang DHP, Holtslag AAM (1996) Evaluation and model impacts of alternative boundary-layer height
824 formulations. *Bound-Lay Meteorol* 81:245–269

825 Vögtlin RM, Kossmann M, Güsten H, Heinrich G, Fiedler F, Corsmeier U, Kalthoff N (1996) Transport of trace-
826 gases from the Upper Rhine valley to a mountain site in the northern Black Forest. *Phys Chem Earth*
827 21:425–428

828 Wang XY, Wang KC (2014) Estimation of atmospheric mixing layer height from radiosonde data. *Atmos Meas*
829 *Tech* 7:1701–1709

830 Weiss-Penzias P, Jaffe DA, Swartzendruber P, Dennison JB, Chand D, Hafner W, Prestbo E (2006) Observations of
831 Asian air pollution in the free troposphere at Mount Bachelor Observatory during the spring of 2004. *J*
832 *Geophys Res* 111(D10304)

833 Whiteman CD, Bian X, Zhong S (1999) Wintertime evolution of the temperature inversion in the Colorado Plateau
834 Basin. *J Appl Meteor* 38:1103–1117

835 Wunderli S, Gehrig R (1990) Surface ozone in rural, urban and alpine regions of Switzerland. *Atmos Environ*
836 24a(10):2641–2646

837 Zardi D, Whiteman CD (2013) Diurnal mountain wind systems. In: Chow FK, De Wekker SFJ, Snyder BJ (eds)
838 Mountain weather research and forecasting. Recent progress and current challenges, Springer, Berlin, pp
839 261–290

840 Zaveri RA, Saylor RD, Peters LK, McNider R, Song A (1995) A model investigation of summertime diurnal ozone
841 behavior in rural mountainous locations. *Atmos Environ* 29(9):1043–1065

842 Zellwegger C, Forrer J, Hofer P, Nyeki S, Schwarzenbach B, Weingartner E, Ammann M, Baltensperger U (2003)
843 Partitioning of reactive nitrogen (NO_y) and dependence on meteorological conditions in the lower free
844 troposphere. *Atmos Chem Phys* 3:779–796

845 Zhu CS, Cao JJ, Xu BQ, Huang RJ, Wang P, Ho KF, Shen ZX, Liu SX, Han YM, Tie XX, Zhao ZZ, Chen LWA
846 (2016) Black carbon aerosols at Mt. Muztagh Ata, a high-altitude location in the Western Tibetan Plateau.
847 *Aerosol Air Qual Res* 16:752–763.